BBA - Molecular and Cell Biology of Lipids 1865 (2020) 158675

Contents lists available at ScienceDirect

BBA - Molecular and Cell Biology of Lipids

journal homepage: www.elsevier.com/locate/bbalip

Inhibitory effects of ceramide kinase on Rac1 activation, lamellipodium formation, cell migration, and metastasis of A549 lung cancer cells

Satoshi Tomizawa[a], Mizuki Tamori[a], Ai Tanaka[a], Naoya Utsumi[a], Hiromi Sato[b], Hiroto Hatakeyama[b], Akihiro Hisaka[b], Takafumi Kohama[a,c], Kazuyuki Yamagata[a], Takuya Honda[a], Hiroyuki Nakamura[a,*], Toshihiko Murayama[a]

[a] Laboratory of Chemical Pharmacology, Graduate School of Pharmaceutical Sciences, Chiba University, 1-8-1 Inohana, Chuo-ku, Chiba 260-8675, Japan
[b] Laboratory of Clinical Pharmacology and Pharmacometrics, Graduate School of Pharmaceutical Sciences, Chiba University, 1-8-1 Inohana, Chuo-ku, Chiba 260-8675, Japan
[c] Research Coordination Group, Research Management Department, Daiichi Sankyo RD Novare Co., Ltd., 1016-13 Kitakasai, Edogawa-ku, Tokyo 134-8630, Japan

ARTICLE INFO

Keywords:
Sphingolipids
Ceramide-1-phosphate
Cell movement

ABSTRACT

Ceramide kinase (CerK) phosphorylates ceramide to ceramide-1-phosphate (C1P), a bioactive sphingolipid. Since the mechanisms responsible for regulating the proliferation and migration/metastasis of cancer cells by the CerK/C1P pathway remain unclear, we conducted the present study. The knockdown of CerK in A549 lung and MCF-7 breast cancer cells (shCerK cells) increased the formation of lamellipodia, which are membrane protrusions coupled with cell migration. Mouse embryonic fibroblasts prepared from CerK-null mice also showed an enhanced formation of lamellipodia. The overexpression of CerK inhibited lamellipodium formation in A549 cells. The knockdown of CerK increased the number of cells having lamellipodia with Rac1 and the levels of active Rac1-GTP form, whereas the overexpression of CerK decreased them. CerK was located in lamellipodia after the epidermal growth factor treatment, indicating that CerK functioned there to inhibit Rac1. The migration of A549 cells was negatively regulated by CerK. An intravenous injection of A549-shCerK cells into nude mice resulted in markedly stronger metastatic responses in the lungs than an injection of control cells. The *in vitro* growth of A549 cells and *in vivo* expansion after the injection into mouse flanks were not affected by the CerK knockdown. These results suggest that the activation of CerK/C1P pathway has inhibitory roles on lamellipodium formation, migration, and metastasis of A549 lung cancer cells.

1. Introduction

Enhancements in the migration/invasion abilities of cells are some of the key factors regulating cancer metastasis. Cell migration and invasion involve multiple and well-coordinated processes, and actin assembly at the cell front drives the extension of membrane protrusions, called lamellipodia, filopodia, and invadopodia, ultimately resulting in cell movement [1–3]. Lamellipodia and filopodia are characterized by sheet-like and needle-like membrane protrusions, respectively, and the formation of lamellipodia at cell edges is widely accepted to be critical for directional cell migration. The formation of membrane protrusions and cell migration are regulated by Rho family small G proteins, such as Cdc42, Rac1, and RhoA [1–3]. The formation of lamellipodia and filopodia is mainly regulated by Rac1 and by both Rac1 and Cdc42, respectively, while stress fiber-related events, including cell contraction and tail retraction, are mainly regulated by RhoA [2,3]. In many cells, including human lung adenocarcinoma A549 cells and human breast cancer MCF-7 cells, the formation of lamellipodia is known to be regulated by Rac1 [3–5].

Ceramide-1-phosphate (C1P), an anionic sphingolipid, is formed by

Abbreviations: C1P, ceramide-1-phosphate; CerK, ceramide kinase; PM, plasma membrane; MEFs, mouse embryonic fibroblasts; SphKs, sphingosine kinases; S1P, sphingosine-1-phosphate; EGF, epidermal growth factor; NVP-231, N-[2-(benzoylamino)-6-benzothiazolyl]-ricyclo[3.3.1.13,7] decane-1-carboxamide; PGE_2, prostaglandin E_2; NSC23766, N6-[2-[[4-(diethylamino)-1-methylbutyl]amino]-6-methyl-4-pyrimidinyl]-2-methyl-4,6-quinolinediamine; Dil, 1,1′-dioctadecyl-3,3,3′,3′-tetramethylindocarbocyanine; DMEM, Dulbecco's modified Eagle's medium; GFP, green fluorescent protein; GAPDH, glyceraldehyde-3-phosphate dehydrogenase; ERM, ezrin/radixin/moesin; NBD, N-7-(4-nitrobezo-2-oxa-1,3-diazole)

* Corresponding author at: Laboratory of Chemical Pharmacology, Graduate School of Pharmaceutical Sciences, Chiba University, Inohana 1-8-1, Chuo-ku, Chiba 260-6875, Japan.
E-mail address: nakahiro@faculty.chiba-u.jp (H. Nakamura).

https://doi.org/10.1016/j.bbalip.2020.158675
Received 30 July 2019; Received in revised form 30 January 2020; Accepted 22 February 2020
Available online 26 February 2020

the direct phosphorylation of ceramide by ceramide kinase (CerK), which was cloned by Kohama and Spiegel's group [6]. C1P is formed in cellular organelles/membranes, including the Golgi complex and plasma membrane (PM), by CerK [7,8], and is then transported by the C1P transfer protein and/or vesicular trafficking to the PM and other membrane fractions [9]. C1P functions both intracellularly and extracellularly [7–11]. Previous studies demonstrated that a treatment with C1P induced and/or enhanced migration of various cells, including fibroblasts, macrophages, and pancreatic cancer cells, and C1P-induced signaling pathways, such as putative C1P receptors and various kinases, have been proposed to regulate cell migration [10–13]. C1P was shown to be up-regulated and released in damaged organs/tissues, and then promoted the migration of multipotent stromal and progenitor cells to damaged organs in order to accelerate their vascularization [14]. An analysis of the gene expression profiles of women with breast cancer revealed that the up-regulated expression of CerK is associated with an increased risk of the recurrence of cancer [15]. These findings showed that elevated C1P levels stimulate cell migration/invasion, either intracellularly or extracellularly. However, Wijesinghe et al. [16] reported an inhibitory role for the CerK/C1P pathway in cell migration; primary mouse embryonic fibroblasts (MEFs) from CerK-null mice migrated faster with a highly random pattern in contrast to their wild-type counterparts. Thus, the role of the CerK/C1P pathway in cell migration remains a challenge to be solved.

The CerK/C1P pathway is one of multiple ceramide metabolic pathways, and, thus, modifications to the pathway in cells may affect other ceramide metabolites, including ceramide, sphingomyelin, and sphingosine. For instance, sphingosine is phosphorylated by sphingosine kinases (SphKs), and the sphingosine-1-phosphate (S1P) formed acts as an activator of S1P receptors [17,18], and the SphK/S1P pathway was involved in the epidermal growth factor (EGF)-induced formation of lamellipodia and/or cell migration in MCF-7 and HeLa cells [19–22]. We recently demonstrated that C1P directly bound with and activated SphK-1 [23]. Thus, the precise mechanisms responsible for lamellipodium formation and cell migration regulated by the CerK/C1P pathway should be elucidated in detail. In the present study, we examined the effects of the molecular inhibition and overexpression of CerK on migration-related events. The results obtained showed that activation of the CerK/C1P pathway reduced the levels of the Rac1-GTP form as well as the formation of lamellipodia in A549 and MCF-7 cells, and negatively regulated both the migration of A549 cells *in vitro* and metastasis of cells *in vivo*. We would like to discuss the suppressive role of the CerK/C1P pathway for migration-related events, the results obtained in this experiment, with reference to previously reported data from other groups that show the stimulatory role of the pathway.

2. Materials and methods

2.1. Materials

N-[2-(benzoylamino)-6-benzothiazolyl]-ricyclo[3.3.1.13,7] decane-1-carboxamide (NVP-231, an inhibitor of CerK) and prostaglandin E_2 (PGE_2) were from Cayman (Ann Arbor, MI, USA). EGF was from R&D Systems (recombinant, Minneapolis, MN). C1P (C16-fatty acid form) was from Avanti Polar Lipids (Alabaster, AL). N6-[2-[[4-(diethylamino)-1-methylbutyl]amino]-6-methyl-4-pyrimidinyl]-2-methyl-4,6-quinolinediamine (NSC23766 trihydrochloride, an inhibitor of Rac1) was from Sigma-Aldrich (St. Louis, MO). 1,1′-dioctadecyl-3,3,3′,3′-tetramethylindocarbocyanine (Dil) and other chemicals were from Wako (Tokyo, Japan). The concentrations of NVP-231 and NSC23766 used in the present study were the same as those reported previously [23–25].

2.2. Cells

Epithelium-derived A549 human lung adenocarcinoma cells (RCB0098; Riken Cell Bank, Tsukuba, Japan) and MCF-7 human breast cancer cells (American Type Culture Collection, Manassas, VA) were cultured in Dulbecco's modified Eagle's medium (DMEM) containing 10% serum as described previously [23,26]. A549 and MCF-7 cells at passages from 3 to 8 were used for each experiment. Cell passage was numbered first after frozen cells were thawed and grown in culture, and cells were passaged at 70–80% confluency. In many experiments including assays for cell migration *in vitro* and metastatic response *in vivo*, we used A549 cells. Previously we confirmed that A549 cells used showed the expected responses coupled with an epithelial-mesenchymal transition after stimulation [27]. Wild-type and CerK-null mice were prepared from $CerK^{(+/-)}$ mice (heterozygous C57BL/6J) and housed as described previously [28]. MEFs were isolated from 13- or 14-day pregnant mice and maintained for five or fewer passages in DMEM supplemented with 10% serum.

2.3. Plasmids

The pMXs-U6-Puro retroviral vector and pCMV-VSV-G envelope vector were gifts from Dr. Kitamura (University of Tokyo, Japan). The knockdown of CerK was performed with short hairpin RNA (shRNA) to silence CerK (shCerK; target sequence GGACAAGGCAAGCGGATAT). A shRNA recognizing luciferase (shLuc) was used as a control [23]. The nucleotides for shRNA were annealed and subcloned into the *Bam*HI/*Eco*RI sites of the pMXs-U6-Puro retroviral vector. To construct green fluorescent protein (GFP)-tagged CerK (CerK-GFP), complementary DNA (cDNA) encoding human CerK (a gift from Daiichi-Sankyo, Co., Ltd., Tokyo, Japan) was amplified by PCR using the forward primer 5′-TAAAAGATCTCGGAGATGGGGGCGA-3′, and a reverse primer 5′-TATAGGAATTCCGCTGTGTGAGTCTGGC-3′, and this amplification product was cloned into the pEGFP-N1 vector at *Bgl*II/*Eco*RI sites. The kinase dead mutant of CerK-GFP (CerK-G198D-GFP) and shRNA-resistant CerK-GFP (CerK*-GFP) were created by PCR using CerK-GFP as a template with the forward primer 5′-CTGTGTCGGCGGAGATGATATG TTCAGCGAGGTGC-3′ and the reverse primer 5′-GCACCTCGCTGAACA TATCATCTCCGCCGACACAG-3′, and the forward primer 5′-GTTTGGA GGAAAAGGTCAGGGCAAGCGGATATA-3′ and the reverse primer 5′-TATATCCGCTTGCCCTGACCTTTTCCTCCAAAC-3′, respectively.

2.4. Retroviral expression and transient transfection of cells

The Plat-GP packaging cell line (a gift from Dr. Kitamura) was cultured in DMEM containing 10% fetal bovine serum. Plat-GP cells were transfected with retroviral vectors and the pCMV-VSV-G envelope vector using a Lipofectamine reagent according to the manufacturer's instructions (Invitrogen, Carlsbad, CA). Retrovirus-containing supernatants were collected 48 h after transfection. A549 or MCF-7 cells were seeded onto 12-mm glass-bottomed dishes at a density of 1×10^4 cells (for phalloidin staining) or 100-mm dishes at a density of 5×10^5 cells (for Rac1 and migration assays), and then transiently transfected with 0.5 μg or 4 μg of plasmid DNAs, respectively, using Lipofectamine2000 (Invitrogen) and OPTI-MEM (Invitrogen) following the manufacturer's instructions.

2.5. Knockdown of CerK

In order to establish a stable CerK knockdown cell line, cells were cultured with retroviral supernatants containing shCerK with 8 μg/mL polybrene for 8 h and then selected in 1 μg/mL puromycin. The knockdown of CerK was confirmed by measuring the levels of CerK mRNA and the activity to form C1P (Fig. 1A).

2.6. Analysis of lamellipodium formation

Cells growing on glass-bottomed dishes were cultured with 10% serum for approximately 24 h. Serum-starved cells were used for the treatment with EGF: cells were cultured on medium without serum for

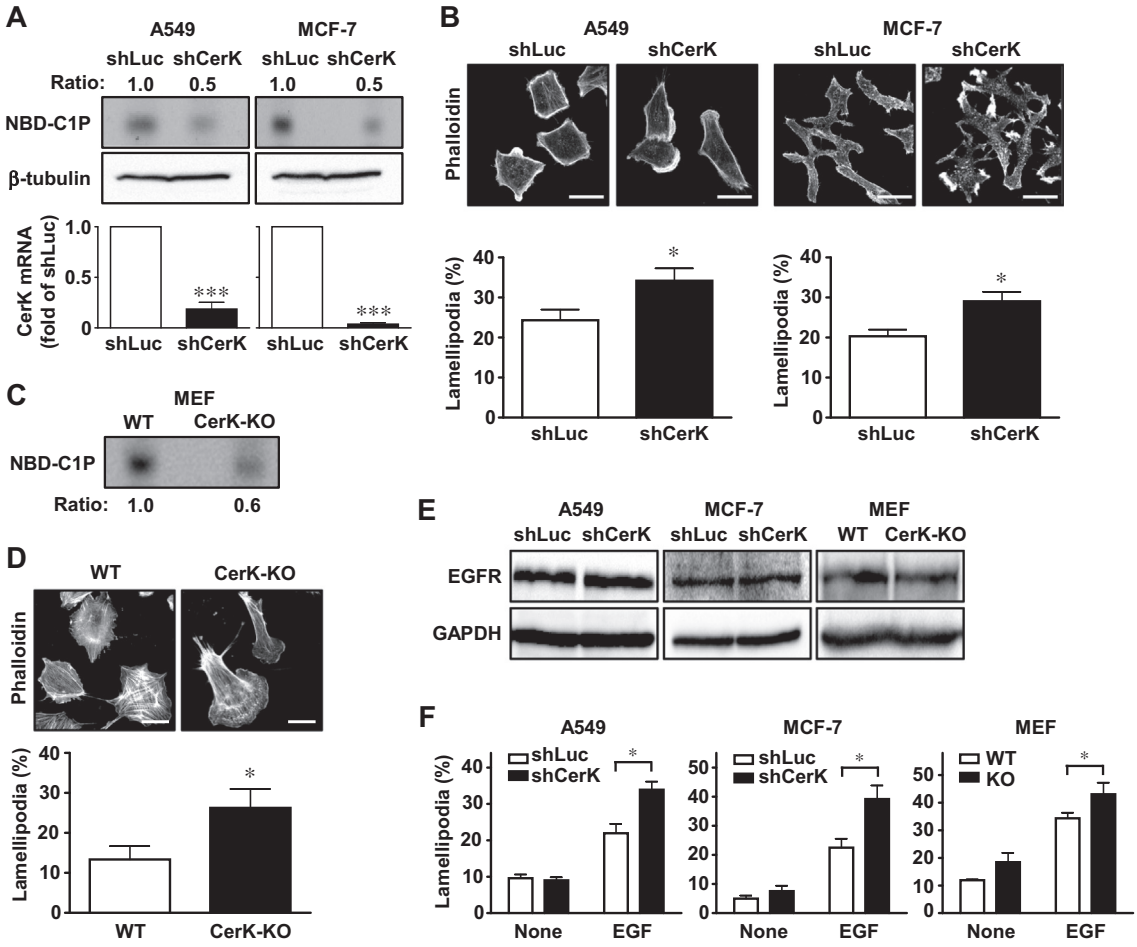

Fig. 1. Effects of the CerK knockdown/knockout on the formation of lamellipodia. In A, A549 cells and MCF-7 cells were transfected with shCerK or shLuciferase (shLuc, control) plasmids, and the CerK knockdown was confirmed by two assays: the formation of NBD-C1P in cells incubated with NBD-ceramide and mRNA levels of CerK. In B, cells were cultured with serum for 24 h, and cell morphology was observed with phalloidin staining. Typical images were shown in the upper panels and quantitative data, the percentages of cells having lamellipodia, were shown in the lower panels. In C and D, MEFs prepared from CerK-null (CerK-KO) mice and wild-type (WT) mice were used. In A and C, the values of NBD-C1P in shCerK cells and CerK-KO cells were shown as the ratio to the control. In E, the respective cells were cultured without serum for 24 h and then analyzed for the levels of EGF receptors (EGFR) and glyceraldehyde-3-phosphate dehydrogenase (GAPDH). In F, the formation of lamellipodia was measured 3 min after the treatment with 20 ng/mL of EGF. Quantitative data are the means ± S.D. of 3–4 independent experiments. *$P < 0.05$, significantly different from the control, A549- and MCF-7-shLuc cells, or wild-type MEFs. Scale bar, 10 μm.

at least 24 h and treated with 20 ng/mL of EGF for 3 or 5 min. After the cultivation or treatment, cells were washed with PBS twice and fixed with 4% paraformaldehyde for 15 min. For Dil staining, cells were treated with 1 μM Dil for 20 min in culture medium before fixation of the cells. Fixed cells were further treated with 0.1% Triton X-100 for 20 min followed by staining with tetramethylrhodamine isothiocyanate-conjugated phalloidin (phalloidin-TRITC) (Sigma-Aldrich) or phalloidin-iFluor 488 reagent (abcam) for 40 min. In the analysis of membrane protrusions, including lamellipodia, samples were examined by confocal microscopy. Lamellipodia are thin and sheet-like protrusions/extensions at the edge of cells that contain a dynamic array of actin filaments and are characterized by the enrichment of phalloidin-sensitive F-actin. The morphological characteristics of lamellipodium including their breadth vary depending on cell type and conditions [1,2,29]. We defined the protrusions having the following characteristics as lamellipodia formed in each cell; areas with visualized F-actin were 1 μm or more in breadth and 0.3 μm or more in vertical in A549 cells; those were 0.5 μm or more in breadth and 0.3 μm or more in vertical in MCF-7 cells. In the case of MEFs, wide protrusions with visualized F-actin were clearly outward from the initial cell periphery, thus defined as lamellipodia. The formation of lamellipodia was assessed by the blinded quantification of microscopy (20–30 cells per view, 2–3 views per experiment, and three representative independent experiments, each sample of > 150 cells). Confocal laser microscopy was performed using a FV500-IX confocal microscope (Olympus, Tokyo, Japan). Two investigators independently assessed the formation of lamellipodia.

2.7. Analysis of CerK-GFP localization in cells

Cells were plated onto 25-mm circular glass coverslips in six-well plates (2×10^5 cells/well), and plasmid DNA (1 μg/well) was transfected using Lipofectamine2000 and OPTI-MEM following the manufacturer's instructions. After 24 h of transfection, cells were washed on the coverslips with HBSS. For fixed-cell imaging, cells were fixed with 4% paraformaldehyde for 15 min. For live-cell imaging, the cells onto the coverslip was placed into a metal chamber (Atto, Invitrogen) and examined on an inverted microscope in 1 mL of HBSS. EGF was dissolved and added to 200 μL buffer removed from the cells. The localization of CerK-GFP was monitored using time-lapse imaging. Confocal images were obtained with a Zeiss LSM 780 laser confocal microscope (Carl Zeiss) using a 63 × 1.4-numerical-aperture plan-apochromatic objective.

2.8. Western blotting

The following antibodies (1:1000–1:3000) were used: anti-β-tubulin antibody (10G10, Lot. 5401, Wako); anti-glyceraldehyde-3-phosphate dehydrogenase (GAPDH) antibody (5A12, Wako, Osaka, Japan); anti-EGF receptor and anti-GFP antibodies (#1005 and B-2, respectively, Santa Cruz); anti-Rac1 antibody (Merck Millipore, Burlington, CA); anti-phospho-ERM (ezrin/radixin/moesin) antibody (41A3, against $E^{The567}/R^{The564}/M^{The558}$, Cell Signaling); anti-ezrin antibody (DSHB, Iowa, IA); and anti-rabbit and anti-mouse IgG horseradish peroxidase antibodies (GE Healthcare, Chicago, IL). Immunoreactive bands were visualized using a chemiluminescent reagent, the clarify Western ECL substrate (Bio-Rad, Hercules, CA). Results were analyzed using the image analyzer ChemiDoc XRS Plus (Bio-Rad). The intensity of chemiluminescence was measured using ImageJ Software (NIH).

2.9. Quantitative real-time PCR

Total RNAs were isolated with the ISOGENII (NIPPON GENE). cDNAs were prepared using the ReverTra Ace qPCR RT Master Mix with gDNA Remover (Toyobo). We used the following primers for PCR: CerK, (sense) 5′-AGTCCACCACAACAGCAC-3′ and (antisense) 5′-GAGGAAG GTCTTTAAACCTG-3′; and β-actin, (sense) 5′-AGCGAGCATCCCCCAAA GTT-3′ and (anti-sense) 5′-GGGCACGAAGGCTCATCATT-3′. qPCR was performed using the PowerUp™ SYBR® Green Master Mix (Applied biosystems). Reactions were run with the Eco Real-Time PCR System (Illumina, San Diego, CA). The following thermal profile was used for all reactions: an initial melting step of 95 °C for 1 min, followed by 40 cycles of a 15 s 95 °C melting step, and a 58 °C annealing step for 45 s.

2.10. Quantification of CerK activity

CerK activity in intact cells was measured using N-[7-(4-nitrobezo-2-oxa-1,3-diazole)] (NBD)-labeled-6-aminocaproyl-D-sphingosine (NBD-ceramide, Molecular Probes, Eugene, OR) as a substrate, as described previously [23,26]. Briefly, the cells were incubated with 10 μM NBD-ceramide for 120 min, and ceramide metabolites, including NBD-C1P, were analyzed on a TLC Silica Gel-60 plate. In the quantitative analysis of NBD-C1P, various amounts (0–20 pmol) of standard NBD-ceramide were spotted in the upper area of the plate after separation by TLC. The fluorescence intensity of NBD-C1P was measured with LAS1000-Plus (Fuji-film, Tokyo, Japan; 470-nm excitation and 515-nm emission).

2.11. Analyses of Rac1 localization in cells and active Rac1

A549 cells grown on 35-mm glass-bottomed dishes were fixed at room temperature for 15 min with 4% paraformaldehyde in PBS and then washed with PBS. Cells were permeabilized and blocked for 1 h with PBS containing 0.3% saponin and 3% albumin. Cells were incubated with the anti-Rac1 antibody (1:300, Merck Millipore) in PBS containing 3% albumin for 3 h. After washing with PBS, cells were incubated with Alexa488-conjugated anti-IgG antibodies (Invitrogen) in PBS containing 3% albumin for 1 h. Cells were counted as having translocated Rac1 in lamellipodia when there was an increase in the visualized accumulation of fluorescence in lamellipodia. The area (0.3 × 0.3 μm) showing 2-fold or more brightness compared to the next area was defined as localization of Rac1. The assay was performed in accordance with the description shown in the analysis of lamellipodium formation by blinded quantification and two investigators. Active Rac1 pull-down assays were performed using the Rac1-activation kit (17–283, Merck Millipore) following the manufacturer's instructions. Briefly, cells cultured in 100-mm dishes were washed twice with ice-cold PBS and lysed in 0.5 mL lysis buffer (25 mM HEPES, pH 7.5, 150 mM NaCl, 1% Igepal CA-630, 10 mM $MgCl_2$, 1 mM EDTA, 2% glycerol, 10 μg/mL leupeptin, 10 μg/mL aprotinin, and 1 mM NaF). Lysates were incubated with PAK-1 agarose (10 μg) at 4 °C for 1 h with rotation. Beads were washed three times in lysis buffer and resuspended in Laemmli buffer. Rac1 binding was detected by Western Blotting.

2.12. Assays for cell migration and proliferation

Cell migration was examined using two assays. In the trans-well assay, the Costar Transwell kit (#3422, Corning, New York, NY) with 8-μm pores was used. A549 cells (5×10^4 cells) were seeded in the upper chambers supplemented with 100 μL of serum-free DMEM. The lower chambers were supplemented with 600 μL of DMEM containing 10% serum, and cells were cultured for 6 h. Cells that had migrated through the filter membrane to the lower chamber were stained by 1% crystal violet solution after fixation with 4% paraformaldehyde. Cells in 5 views per experiment were counted using a microscope (Nikon ECLIPSE-TS100, Tokyo), and three or four independent experiments were performed. In the wound healing assay, cells plated on 12-well plates were cultured to form a sub-confluent monolayer, scratched with a 200-μL pipette tip to create a wound, and incubated in fresh medium containing 10% serum after washing. Pictures were taken every 6 h, and images were analyzed using the program Adobe Photoshop. The percentage of the non-recovered wound area (open wound) was calculated by dividing the non-covered area after a respective 6-h interval by the initial wound area at the indicated periods. For cell proliferation assay, cells (3×10^4 cells) were seeded on a 6-well plate and cultured with DMEM containing 10% serum.

2.13. Tumor metastasis and tumorigenesis assays in nude mice

Male BALB/cSlc-*nu/nu* mice were purchased from SLC Co. (Shizuoka, Japan), and housed under pathogen-free conditions and cared for according to the animal care guidelines of Chiba University. Experiments were performed according to an animal protocol approved by the Animal Welfare Committee of Chiba University. In the tumor metastasis assay, A549-shLuc cells and A549-shCerk cells (2×10^6 cells/100 μL/mouse in PBS) were injected into nude mice (7 week-old) through the lateral tail vein with a 30G needle. After 34 days (Fig. 6) or 28 days (Suppl. Fig. 5), the lungs of sacrificed mice were evaluated for weight and metastatic nodules. Metastatic nodules in lungs after fixation with Bouin's fluid were scored under a stereoscopic microscope. In the tumorigenesis assay, tumors were incubated in male BALB/c nude mice (5 week-old) by a subcutaneous inoculation of the cells [1×10^6 cells/200 μL/mouse in a mixed solution (50% Matrigel (Corning, New York, NY) and 50% HBSS)] into the right and left dorsal flanks. The longitudinal (L) and transverse (T) diameters and heights (H) of tumors in the two flanks in a mouse were measured every 3 days, and the tumor volume was calculated using the following formula: volume = $\pi/6 \times L \times T \times H$. Forty-two days after implantation, mice were killed, tumors dissected, and tumor weights measured.

2.14. Quantitative analyses of sphingolipids

Cells cultured in three 100-mm dishes were washed twice with ice-cold PBS and harvested by scraping in PBS. After centrifugation (3000 ×*g*, 4 °C, 5 min), cell pellets were stored at −80 °C. Quantitative analyses of sphingolipids were performed by Virginia Commonwealth University Lipidomics/Metabolomics Core (VA, USA).

2.15. Statistical analysis

Data for Rac1-GTP/Rac1 levels and cell migration were expressed as fold changes from the control. The control values in Rac1-GTP/Rac1 levels and cell migration were dependent on each experiment, and the standard deviations in the control were approximately plus/minus 30–40%. Thus, we did not show standard deviations in the control in

Figures. Data are means ± S.D. for the indicated number (n) of independent experiments. The Student's *t*-test was used for pair-wise comparisons, and an ANOVA (Non-parametric, Kruskal-Wallis test) followed by Dunn's multiple compartment test GraphPad Prism 5.0 (GraphPad Software, San Diego, CA) for multiple comparisons. A p value < 0.05 was considered to be significant.

3. Results

3.1. Effects of the CerK knockdown on the formation of lamellipodia in cells

We used a shCerK plasmid to knockdown CerK and a shLuciferase (shLuc) plasmid as the control. The extent of the knockdown of CerK was confirmed by two assays: reductions in the formation of NBD-C1P in cells that were incubated with NBD-ceramide for 2 h and in CerK mRNA levels (Fig. 1A). The values of NBD-C1P formation in A549-shCerK cells and MCF-7-shCerK cells were approximately the half of those in the control cells, and whole images of NBD-ceramide metabolites in TLC plates were shown in Supplementary Fig. 1. Cells were then cultured in the presence of 10% serum, and cells having lamellipodia were observed by confocal microscopy. In our confocal images, labeling of A549 cells with the membrane probe Dil showed that the labeling of phalloidin in lamellipodia is not simply due to the thickness of the membrane, because the strong fluorescent signal of phalloidin in A549-shCerK cells having lamellipodia is not colocalized with Dil (Suppl Fig. 2). In A549 and MCF-7 cells, the number of cells having lamellipodia in each shCerK-treated cell line was significantly higher than that in the respective control cell line (Fig. 1B). Similar results were obtained in MEFs prepared from CerK-null mice (Fig. 1C and D). The treatment of cells with EGF has been shown to induce the formation of lamellipodia/filopodia in various cells including A549 and MCF-7 cells [2,4,30]. We then investigated the effects of the CerK knockdown and/or knockout on the EGF-induced formation of lamellipodia. In the measurement of EGF-induced responses, cells were cultured with serum-free medium for 24 h before the EGF treatment. The levels of EGF receptors in cells tested remained unchanged by the CerK knockdown/knockout (Fig. 1E). The treatment with 20 ng/mL of EGF for 3 min markedly increased the number of cells with lamellipodia, and the knockdown/knockout of CerK enhanced EGF responses (Fig. 1F). Images of the EGF-induced formation of lamellipodia in A549 cells and MCF-7 cells were shown in Fig. 3. Under our experimental conditions, the percentage of cells with lamellipodia in serum-starved cells without stimuli was approximately 10%, which was markedly lower than that in cells cultivated with serum (20–30%). In previous studies, the down-regulation of CerK activity inhibited cell proliferation and/or reduced survival in various cells, including A549 and MCF-7 cells [15,31]. Under our experimental conditions, the proliferation rate of A549-shCerK cells was similar to that of control cells in the presence of serum (Fig. 5F), and the knockdown/knockout of CerK did not affect the proliferation of MCF-7 cells and MEFs with serum (data not shown). The pretreatment of A549 cells with 200 nM NVP-231, a selective and potent inhibitor of CerK [24], for 30 min enhanced the formation of lamellipodia by the EGF stimulation. The percentages of cells with lamellipodia were 9.1 ± 0.5% in EGF-treated cells and 15.2 ± 1.4% in NVP-231/EGF-treated cells ($n = 3$, $P < 0.05$).

3.2. Effects of the CerK overexpression on the formation of lamellipodia in A549 cells

A549 cells were transfected with plasmids for CerK-GFP and GFP as the control. The expression of CerK-GFP was confirmed by Western blotting with the anti-GFP antibody and by the increased formation of NBD-C1P (Fig. 2A). A previous study reported that CerK localized to the Golgi complex and endosomal/exosomal compartments in A549 cells [32]. Similarly, CerK-GFP was mainly expressed in punctuate structures and the PM (Fig. 2B). Lamellipodia were observed in 30% of cells cultivated with serum, and the expression of CerK-GFP reduced the percentage of cells with lamellipodia. Under serum-starved conditions, the expression of CerK-GFP also reduced EGF-induced response (Fig. 2C). We constructed a plasmid for CerK-rescue form (CerK*)-GFP, which is shRNA-resistant, and examined the effects of CerK*-GFP on responses in A549-shCerK cells. The expression of CerK*-GFP was confirmed by Western blotting (Fig. 2D) and markedly increased the formation of NBD-C1P in A549-shCerK cells and control A549-shLuc cells. The expression of CerK*-GFP canceled the effects of shCerK on the formation of lamellipodia in cells cultivated with serum (Fig. 2E) and treated with EGF (Fig. 2F). The obtained results shown in Figs. 1 and 2 suggested that activation of the CerK/C1P pathway inhibited the formation of lamellipodia. Next, we examined the effects of CerK-G198D-GFP, a kinase-dead mutant of CerK. Since the expression of CerK-G198D-GFP did not inhibit the formation of NBD-C1P in A549 cells (Fig. 2G), the kinase-dead mutant protein did not appear to act as a dominant-negative form of CerK. The expression of CerK-G198D-GFP did not reduce the formation of lamellipodia in cells cultivated with serum (Fig. 2H) and treated with EGF (data not shown). Therefore, C1P produced by CerK, not CerK protein, appeared to be essential for reducing the formation of lamellipodia in cells.

3.3. Localization of CerK and Rac1 in lamellipodia

Next, we monitored the spatiotemporal localization of CerK in cells before and after the EGF treatment. MCF-7 cells cultivated with serum showed filopodia- and lamellipodia-like protrusions (Fig. 3A), as previously reported [33]. CerK-GFP was localized to the PM including filopodia-like protrusions and punctate structures in the cytoplasm in non-stimulated MCF-7 cells. Upon the EGF stimulation, CerK-GFP was localized in the ruffling membranes formed within 8 min. The localized areas of CerK-GFP after the EGF treatment were consistent with the areas stained with phalloidin in MCF-7 and A549 cells (Fig. 3B and C, respectively); therefore, we concluded that the EGF treatment caused the localization of CerK-GFP to lamellipodia. CerK-G198D-GFP appeared to be localized in the lamellipodia of cells similar to CerK-GFP (Fig. 2H).

The formation of lamellipodia was regulated by Rac1 in many cells including A549 and MCF-7 cells [2–5]. Various stimuli for cell migration including serum caused the translocation of Rac1 in lamellipodia and membrane ruffles in cells [34,35]. In A549-shCerK cells cultivated with serum, Rac1 was localized in the flat protrusions in the PM (Fig. 4A). The number of cells having Rac1-positive protrusions was significantly higher in A549-shCerK cells than in A549-shLuc cells, which is consistent with the results shown in Fig. 1B of the identification of lamellipodia by phalloidin staining. The CerK knockdown also increased the proportion of cells with Rac1-positive protrusions among EGF-treated cells (Fig. 4B), and the expression of CerK-GFP reduced the number of cells with Rac1-positive protrusions in the presence of serum (Fig. 4C) and the EGF stimulation (Fig. 4D). These results suggest that Rac1 was localized in the lamellipodia of cells after a treatment with serum or EGF, and that the CerK knockdown increased the number of cells having lamellipodia accompanied by Rac1. The knockdown and expression of CerK increased and decreased the levels of GTP-bound Rac1, respectively (Fig. 4E and F), while the expression of CerK-G198D-GFP did not change the levels of GTP-bound Rac1 (Fig. 4G). The treatment with NSC23766, an inhibitor of Rac1 [25], markedly reduced the formation of lamellipodia (Fig. 4H and I). The expression of dominant-negative (T17N) Rac1 [34] also reduced the formation of lamellipodia with serum (Fig. 4J) or EGF (Fig. 4K and Suppl. Fig. 3). These results suggest that CerK/C1P decreased the formation of lamellipodia by inhibiting the Rac1 pathway.

3.4. Roles of CerK in the cell migration

The effects of the knockdown or overexpression of CerK on cell

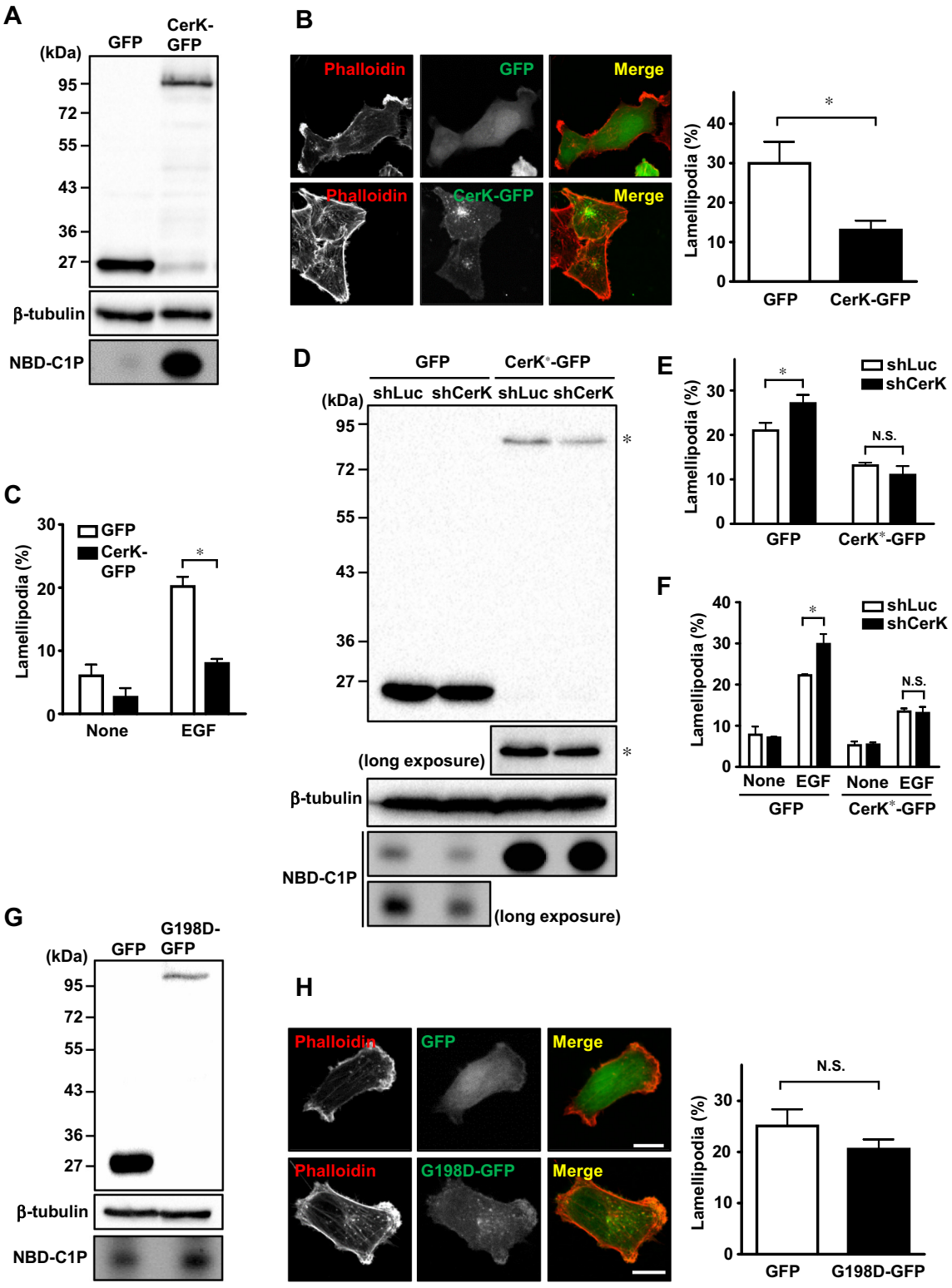

Fig. 2. Effects of CerK overexpression on the formation of lamellipodia. In A, A549 cells were transfected with CerK-GFP and GFP (control) plasmids and analyzed for the levels of CerK-GFP and formation of NBD-C1P. In B, the formation of lamellipodia was observed in cells cultured with serum. Typical images (Left) and quantitative data (Right) were shown. In C, cells after serum starvation were treated with EGF for 3 min, and the formation of lamellipodia was measured. In D-F, A549-shCerK cells and control cells were transfected with CerK-rescue form-GFP (CerK*-GFP) and GFP plasmids. In D, the levels of CerK*-GFP and formation of NBD-C1P were analyzed. In E and F, the formation of lamellipodia was observed in cells cultured with serum (E) and in cells treated with EGF for 3 min after serum starvation (F). In G and H, A549 cells were transfected with plasmids for GFP and CerK-G198D-GFP, a kinase dead mutant of CerK. In G, the levels of CerK-G198D-GFP and formation of NBD-C1P were analyzed. In H, the formation of lamellipodia was observed in cells cultured with serum. Typical images (Left) and quantitative data (Right) were shown. Quantitative data are the means ± S.D. of three independent experiments. *$P < 0.05$, significantly different from control cells, A549-GFP cells, and A549-shLuc cells. Scale bar, 10 μm.

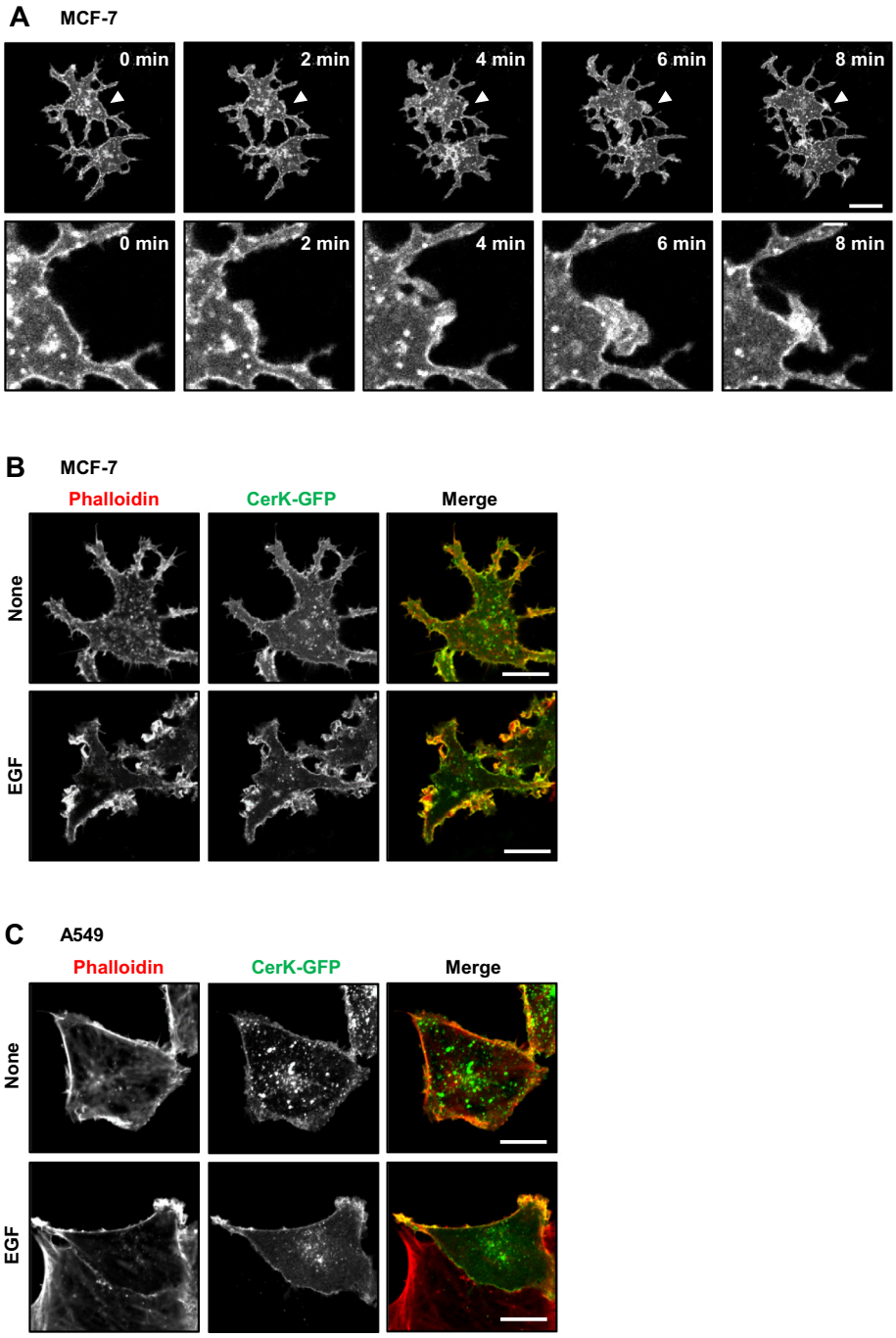

Fig. 3. Accumulation of CerK-GFP in lamellipodia in cells treated with EGF. MCF-7 cells (A and B) and A549 cells (C) were transfected with a CerK-GFP plasmid. In A, GFP-derived fluorescence was chased for the indicated periods after the treatment with 20 ng/mL of EGF. Lamellipodia at the edge of cells were indicated by arrows. In B and C, both cell morphology in a phalloidin staining assay (F-actin, red) and fluorescence derived from CerK-GFP were observed 5 min after the treatment with EGF. Scale bar, 10 μm.

migration were examined using two methods. In the trans-well assay, A549-shCerK cells (Fig. 5A) and A549-CerK-GFP cells (Fig. 5B) showed enhanced and reduced cell migration, respectively. A549-CerK-G198D-GFP cells showed the same migration as control cells (Fig. 5C). The expression of CerK*-GFP (Fig. 5D) and inhibition of Rac1 by the treatment with NSC23766 (Fig. 5E) canceled the enhanced migration of A549-shCerK cells (also see, Suppl. Fig. 4). We then examined the directional cell migration of A549 cells using the wound healing assay. As a pre-step to the assay, we measured the effects of the CerK knockdown on cell proliferation, which is known to increase in response to the sensing of free space after wounding. The proliferation of A549 cells was not affected by the CerK knockdown (Fig. 5F). A monolayer of A549 cells was subjected to a scratch-induced mechanical wound, and cell migration was examined (Fig. 5G). The cell migration of control A549-shLuc cells was relatively unidirectional to close the wound, whereas A549-shCerK cells appeared to migrate in many directions. The total percentages of wound closure were similar in the two cells types (Fig. 5H), whereas the length of the wound edge in A549-shCerK cells at 12 h was significantly longer than that in control cells (Fig. 5I).

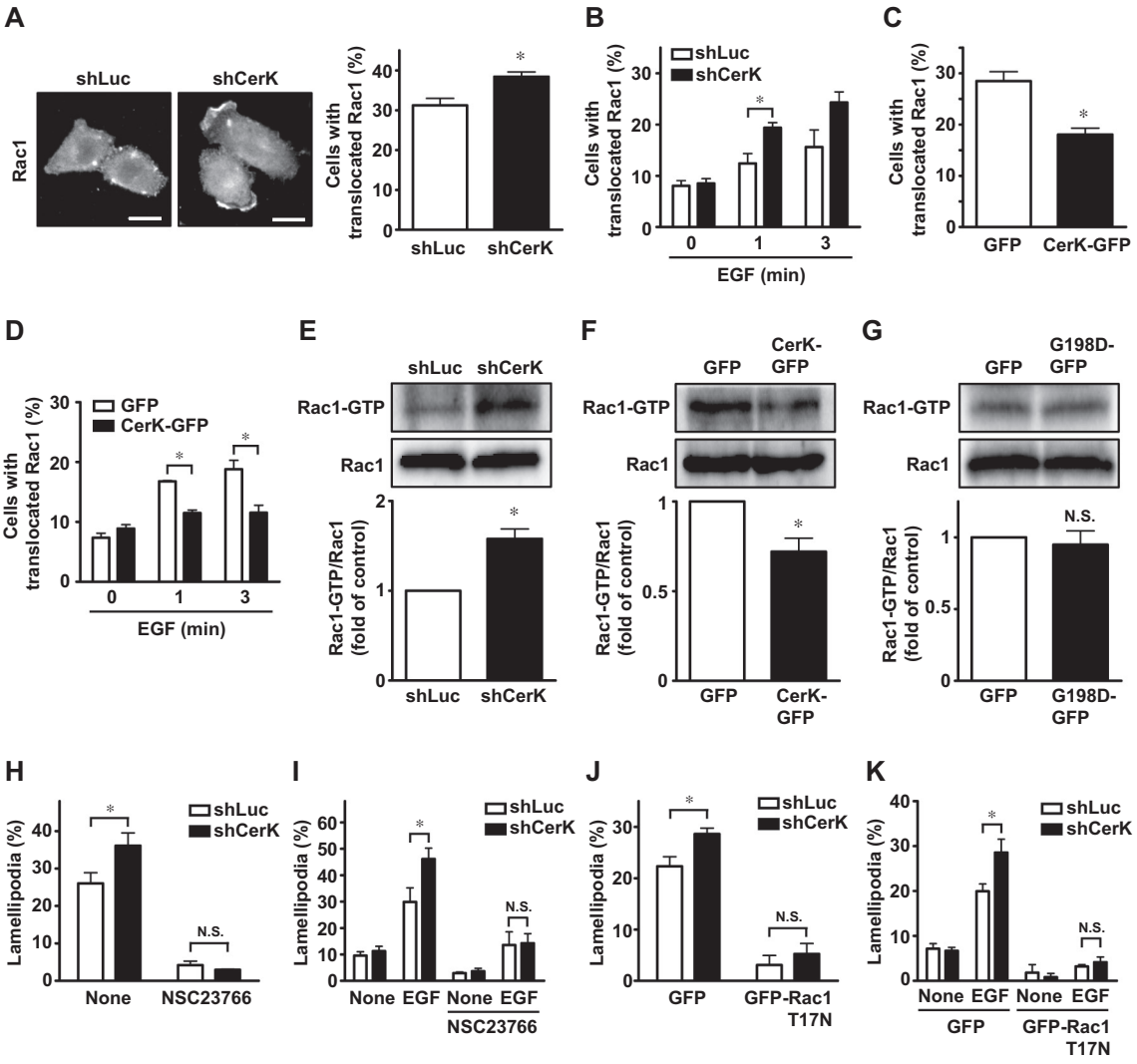

Fig. 4. Role of Rac1 in the formation of lamellipodia and CerK-induced inhibition of Rac1. A549 cells were transfected with shCerK (A, B, E), CerK-GFP (C, D, F), or control (shLuc and GFP) plasmids. Cells were cultivated with serum for 24 h (A, C), and serum-starved cells were treated with 20 ng/mL of EGF for 1 and 3 min (B, D). Cells were stained with the anti-Rac1 antibody and cells with Rac1-positive lamellipodia were defined as cells with translocated Rac1. On the left in A, typical images of cells cultured with serum were shown. In E, F, and G, the levels of Rac1-GTP were analyzed. In G, A549 cells expressing CerK-G198D-GFP, a kinase dead mutant of CerK (G198D), were used. Typical images and quantitative data were shown in the upper and lower panels, respectively. The levels of Rac1-GTP were normalized to those of total Rac1 protein levels. In H–K, the effects of the pharmacological (H and I) and molecular (J and K) inhibition of Rac1 on the formation of lamellipodia were examined. In H and I, cells were treated with vehicle and 100 μM NSC23766, an inhibitor of Rac1, for 1 h before the observation of cell morphology. The respective cells were cultured with serum (H) and serum-starved cells were treated with EGF (I). In J and K, A549 cells were transfected with GFP-Rac1-T17N, a dominant negative mutant of Rac1, and control (GFP) plasmids. The respective cells were cultured with serum (J) and serum-starved cells were treated with EGF (K). Quantitative data are the means ± S.D. of three independent experiments. *$P < 0.05$, significantly different from the control, A549-shLuc cells, and A549-GFP cells. Scale bar, 10 μm.

3.5. Roles of CerK in tumor growth and metastasis of A549 cells in vivo

We investigated the growth and metastasis of A549-shCerK cells in mice. A549-shLuc cells and A549-shCerK cells were injected into the flanks of nude mice to evaluate tumor growth. Time-dependent increases in tumor volumes (Fig. 6A) and tumor weights 42 days after the injection (Fig. 6B) were not affected by the CerK knockdown in A549 cells. The data *in vivo* appeared to be consistent with those *in vitro* (Fig. 5F). Next, cells were injected intravenously into nude mice and the metastasis of cancer cells to the lungs was examined in two independent experiments. Thirty-eight days after the injection (Case I), the sizes of the lungs appeared to be greater (Fig. 6C) and lung weights were significantly greater in mice injected with A549-shCerK cells than in those injected with A549-shLuc cells (Fig. 6D). Changes in body weight were similar in the two groups of mice (Fig. 6E). Lung weights were also significantly ($P < 0.05$) greater in mice injected with A549-shLuc cells than in healthy mice. In another experiment (Case II, 28 days after the injection), the number of metastatic nodules in lungs was counted in mice treated with A549-shCerK cells; it was slightly higher than in mice treated with control cells ($P = 0.16$ by unpaired *t*-test, $n = 6$, respectively, Suppl. Fig. 5). In Case II, total lung weights were 0.23 ± 0.02 g in mice treated with A549-shCerK cells and 0.20 ± 0.01 g in mice treated with control cells. The metastasis of cancer cells to other tissues, including liver, was not observed in either case.

3.6. Cellular sphingolipid levels in A549-shCerK cells

Under our experimental conditions using serum, the levels of C1P subspecies having C14:0, C18:1, and C20:0 as *N*-acyl chains were low at < 1 pmol/mg protein, and the knockdown of CerK reduced the levels

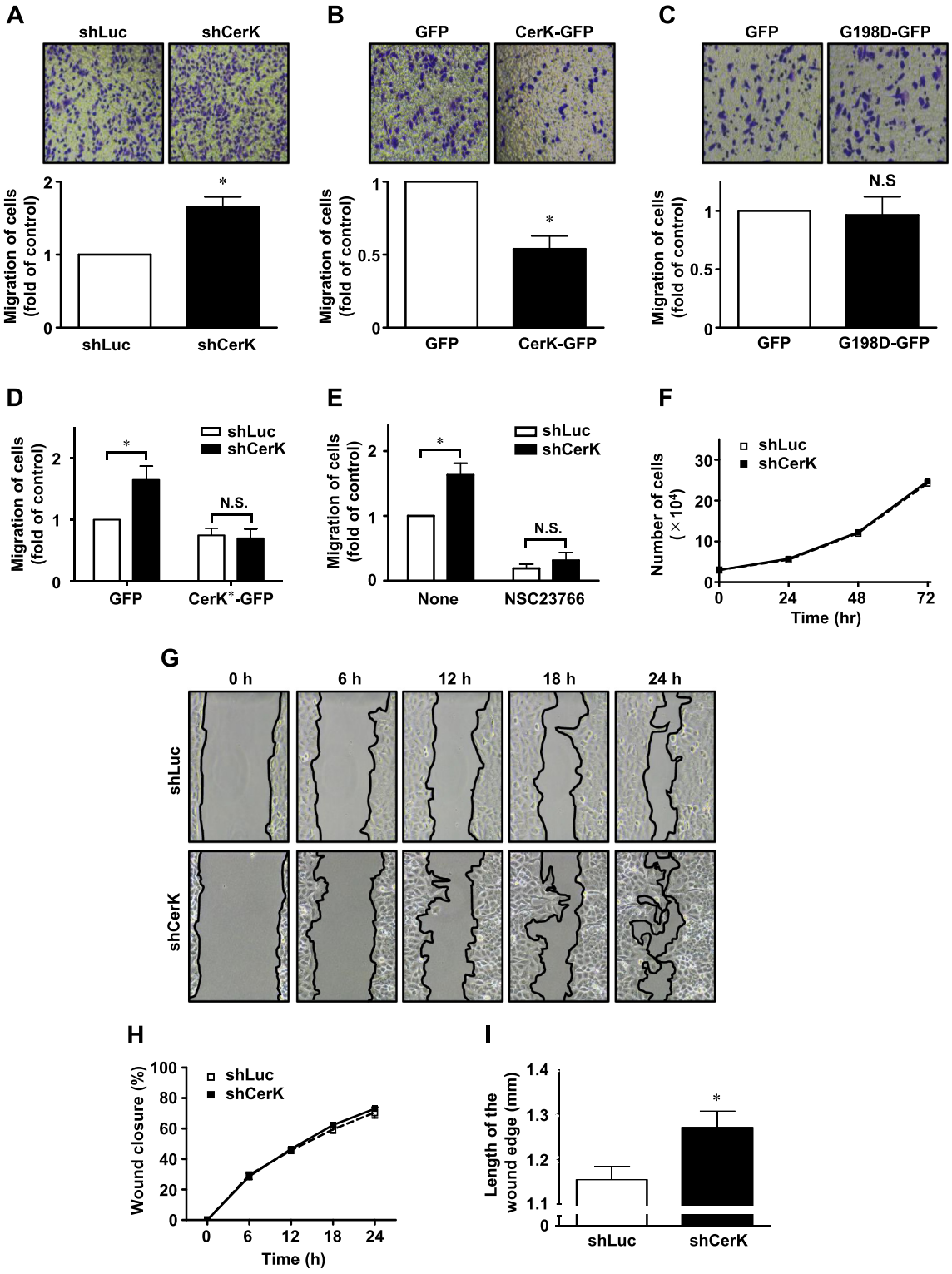

Fig. 5. Effects of the knockdown and overexpression of CerK on the cell migration of A549 cells. The migratory activity of cells was analyzed by the trans-well assay (A–E) and wound healing assay (G–I). The respective modified A549 cells (shCerK cells, CerK-GFP cells, CerK-G198D-GFP cells, A549-shCerK cells expressing CerK*-GFP, and control A549 cells) were used. In A-E, cells were seeded onto polycarbonate filters and then incubated for 24 h in the upper chamber in trans-well plates, and cells that migrated through the filters were stained and counted. In A–C, typical images of migrated cells and quantitative data were shown in the upper and lower panels, respectively. In E, cells were pretreated with vehicle and 100 μM NSC23766 for 1 h before the migration assay. The migration of cells was normalized to that of the respective control cells. In F, the cell proliferation of A549-shCerK cells and control cells on cultured dishes was monitored at the indicated periods. In G-I, the cell migration of A549-shCerK cells was monitored using the wound healing method for the indicated periods. Typical images of cells were shown in G. Wound edges at the respective periods were shown as lines. In H, the quantitative amounts of wound closure were expressed as percentages of the wound dimension (0 h) before cultivation. In I, the lengths (mm) of wound edges 12 h after the migration assay were measured. Quantitative data are the means ± S.D. of three independent experiments. *$P < 0.05$, significantly different from the control, A549-shLuc cells, and A549-GFP cells.

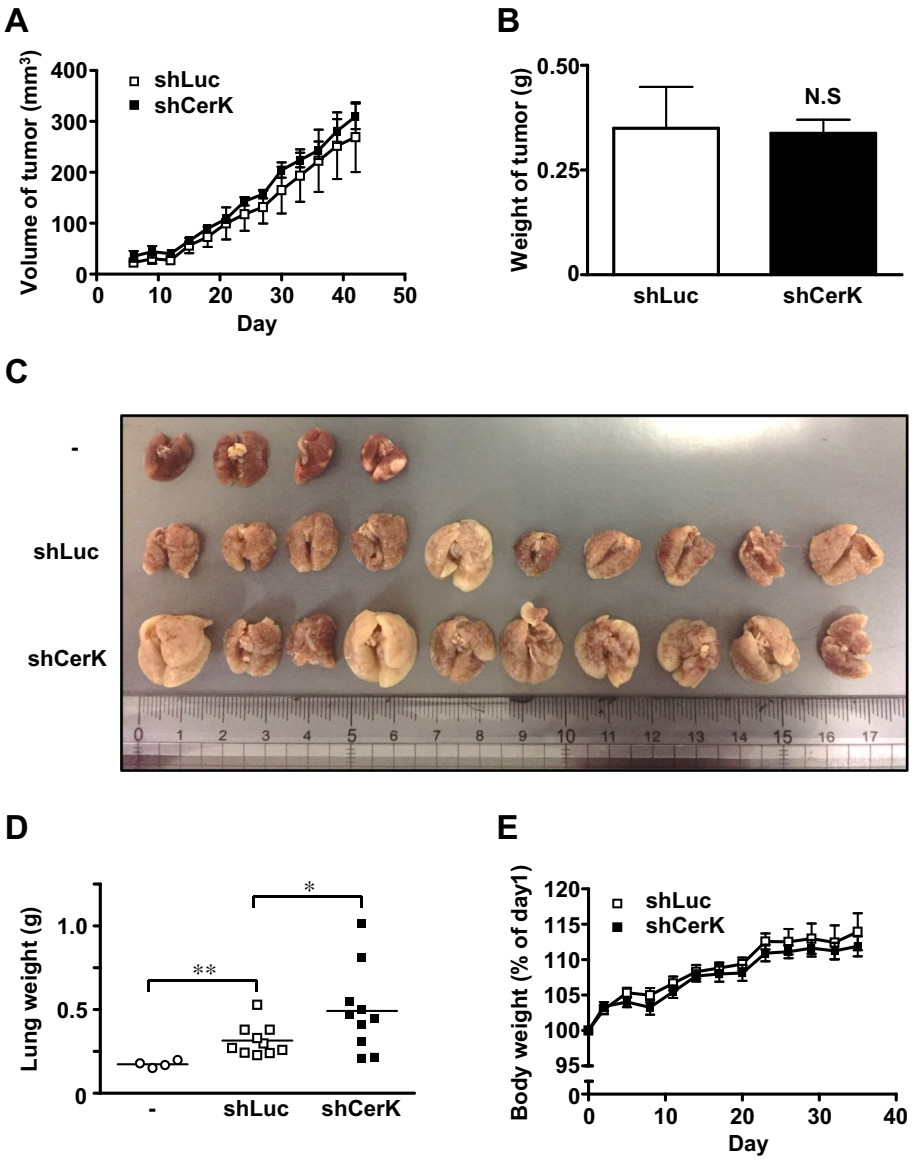

Fig. 6. Effects of the CerK knockdown in A549 cells on tumor growth and metastasis in athymic nude mice. In A and B, tumors were generated by the flank inoculation of A549-shCerK cells and A549-shLuc cells in nude mice (n = 4, respectively). Cells were injected into both the right and left flanks, and the two tumor sizes in a mouse were analyzed. In A, tumor sizes were measured with external calipers and calculated as described in the Materials and methods section. In B, tumor weights were evaluated on day 42. In C–E, the respective cells were injected intravenously into nude mice, and the complete lungs of animals sacrificed on day 34 after the injection were isolated. Images of the lungs were shown in C, and lung weights were measured in D. Changes in body weights were shown in E. Quantitative data are the means ± S.D. of the indicated number of mice. *P < 0.05, significantly different from control A549-shLuc cells.

of these C1P subspecies in A549 cells by 20–45% (Fig. 7A). The levels of C1P having C16:0, C22:0, C26:1, and C26:0 were approximately 1–5 pmol/mg protein, and the CerK knockdown did not affect the levels of these C1P subspecies (Fig. 7B). Consistent with the higher levels of ceramide having C24:1 and C24:0 as *N*-acyl chains (Suppl. Table 1), C24:1 C1P and C24:0 C1P were the main forms of C1P (Fig. 7C). Total C1P levels were not affected by the CerK knockdown in A549 cells, as shown in the immortalized MEFs of CerK-null mice [16]. The levels of ceramide, sphingomyelin, and monohexosylceramide, including total levels (Fig. 7D) and levels irrespective of *N*-acyl chain lengths (Suppl. Table 1), were not affected by the CerK knockdown.

4. Discussion

Our results demonstrated for the first time that C1P generation through CerK suppresses lamellipodium formation in A549 cells, and the CerK/C1P pathway plays an inhibitory role in migration and metastasis of A549 cells *in vitro* and *in vivo*, respectively. Interestingly, slight decreases in several C1P subspecies were detected in A549-shCerK cells, but levels of other C1P species and total C1P were not changed by the CerK knockdown. Many researches show that cell migration was positively regulated by the extracellular application of C1P in various cells including A549 cells [11,14,18,36]. Thus, there may be two apparent contradictions: the unaltered (or hardly altered) C1P levels in A549-shCerK cells and the opposite migratory responses mediated by the CerK/C1P pathway, a stimulation reported in many previous studies and an inhibition shown in the current study and by Wijesinghe et al. [16]. These points were discussed in the following parts, Sections 4.4 and 4.5.

4.1. Enhanced formation of lamellipodia by the CerK knockdown

We showed that the knockdown and overexpression of CerK in A549 cells enhanced and reduced the formation of lamellipodia, respectively, *via* the regulation of Rac1 activity. The CerK knockdown/knockout-induced enhancement of the formation of lamellipodia was observed in MCF-7 cells and MEFs from CerK-null mice. The overexpression of CerK-G198D-GFP, a kinase-dead mutant of CerK, did not affect the formation of lamellipodia, and the pretreatment with NVP-231 enhanced the EGF-induced formation in A549 cells. Thus, we propose an inhibitory role for C1P, at least formed intracellularly, on the formation of lamellipodia in cells. How does C1P regulate the formation of lamellipodia in cells? Rac1 plays an essential role in the organization of the actin cytoskeleton, formation of lamellipodia, and cell migration in

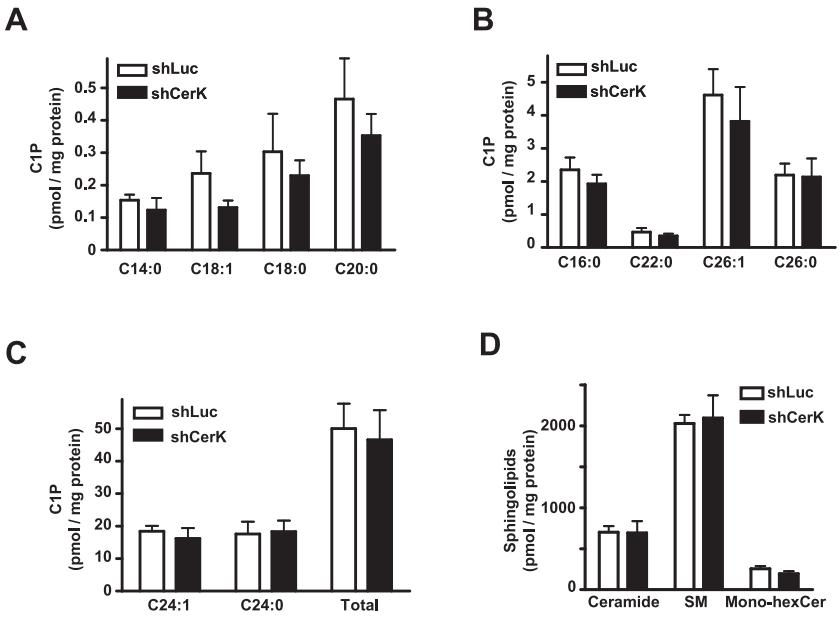

Fig. 7. Effects of the CerK knockdown on cellular levels of C1P subspecies and sphingolipids in A549 cells. Extracted lipids were analyzed as described in the Materials and methods section. Levels of C1P irrespective of *N*-acyl chain lengths were shown in A–C. Total levels of C1P and those of ceramide, sphingomyelin (SM), and monohexosylceramide (Mono-hexCer) were shown in C and D, respectively. The levels of lipids irrespective of *N*-acyl chain lengths and sphingosine analogs were shown in Supplementary Table 1.

various cells [2,3,34,37], and in serum- or EGF-stimulated A549 cells [38]. In the present study, we revealed that the levels of Rac1-GTP, an active form of Rac1, were regulated positively and negatively by the knockdown and overexpression of CerK, respectively. The pharmacological and molecular inhibition of Rac1 markedly inhibited the formation of lamellipodia in cells, while the knockdown of CerK increased the number of cells with lamellipodia co-localized with Rac1. Negatively charged lipids, such as phosphatidylinositols and phosphatidylserine, bind the positively charged polybasic regions in small GTPases, including Rac1, and these lipids also regulate the activities of several GTPase-activating proteins and guanine-nucleotide exchange factors [35]. In migrating MCF-7 cells, the localization of Rac1 at the leading edge of the PM was regulated by phosphatidylinositol-3,4,5-triphosphate [37]. Thus, C1P, a negatively charged lipid, may directly or indirectly inhibit Rac1 functions. Several groups reported the trafficking of CerK to the PM in cells after treatments with Ca^{2+} ionophore [32] and osmotic shock [39]. Treatment of A549 cells with EGF enhanced the accumulation of CerK in lamellipodia, although the treatment did not enhance C1P formation [26]. Thus, EGF-induced localization, not activation, of CerK in lamellipodia appeared to regulate Rac1 function *via* a local formation of C1P. The localization of CerK and Rac1 in lamellipodia, which exert opposing effects on the formation of lamellipodia, may be in harmony to regulate their formation in cells. The N-terminus of CerK bears a pleckstrin homology (PH) domain that can bind with high affinity to certain acid lipids including phosphatidylinositol 4,5-bisphosphate and 3,4,5-triphosphate, and the PH domain of CerK regulates its targeting and sub-cellular localization [8,39]. Acidic lipids and/or negatively charged lipids including phosphatidylinositol 3,4,5-triphosphate have been shown to regulate functions/activities of many proteins regulating actin cytoskeleton [1,37,40]. Thus, acidic lipids in lamellipodia may recruit CerK in there.

4.2. Enhanced migration and metastasis of A549-shCerK cells by the intracellular knockdown of CerK

The arachidonic acid/PGE_2 pathway promoted cell migration in A549 cells [41,42], and this pathway also positively regulated the formation of membrane protrusions and migration in MCF-7 cells [43,44]. C1P acted as a direct activator of group IVA PLA_2 and induced the release of arachidonic acid and formation of prostanoids [7,45]. Since the arachidonic acid/PGE_2 pathway was down-regulated by the knockdown of CerK [16], CerK knockdown-mediated responses, including enhanced cell migration, did not appear to be explained by this pathway. C1P has been shown to directly bind with the annexin A2/11 protein complex existing in/on the PM and enhance the migration/invasion of primary human endothelial cells [36]. The down-regulation of annexin A2 in A549 cells decreased A549 cells-derived tumor growth in mice [46]. In the present study, however, the CerK knockdown of A549 cells increased the sizes and weights of lungs in mice, which reflect the formation of tumors derived from the cells injected intravenously. In another trial (Suppl. Fig. 5), the CerK knockdown slightly increased the formation of metastatic nodules of A549 cells in lungs. Thus, the annexin A2-mediated pathway may be unrelated to our results. A probable regulation of Rac1 induced by the CerK/C1P pathway appeared to be involved in cell migration *in vitro* and metastatic response *in vivo*, in addition to the formation of lamellipodia in cells.

4.3. Possible involvement of other ceramide metabolites other than C1P on A549 cell migration and metastasis

Ceramide is metabolized by various pathways/enzymes besides CerK, therefore, changes in the expression of the CerK protein appeared to affect the levels of ceramide and other ceramide metabolites. In addition, direct interactions have been reported between C1P and the ceramide-related enzymes [23,47]. Thus, our results induced by the CerK knockdown in A549 cells may be caused by these changes in the levels of ceramide and other ceramide metabolites. Ceramide synthesis *via* the activation of ceramide synthase-6 caused the formation of lamellipodia in non-small-cell lung cancer cells and the knockdown of the enzyme decreased cell migration *in vitro* and the metastasis of cancer cells to the lungs after an intravenous injection [48]. However, the accumulation of ceramide decreased the formation of lamellipodia and cell migration in MCF-7 cells [33] and delayed the formation of colonies of PC-3 prostate cancer cells in the lungs after an intravenous injection [49]. The CerK knockdown enhanced the formation of lamellipodia in both A549 and MCF-7 cells in the present study, thus, changes on ceramide levels could not explain our results. The SphK/S1P pathway was shown to be involved in the formation of lamellipodia/filopodia and migration of EGF-treated MCF-7 cells [19,48]. In A549 cells, activation of the S1P receptor up-regulated the expression of EGF receptors and enhanced cell invasion by EGF [17]. Activation of the SphK/S1P pathway and/or an EGF treatment induced the formation of membrane protrusions and/or cell migration *via* the phosphorylation of

ERM proteins, which are actin-interacting proteins, in various cells including A549 and MCF-7 cells [17,19–22,33]. However, neither the expression levels of EGF receptors nor phosphorylation levels in ERM (Suppl. Fig. 6) in A549 cells were affected by the CerK knockdown in the present study. The precise role of the SphK/S1P pathway on the enhanced formation of lamellipodia and migration induced by the CerK knockdown in A549 cells remained to be solved.

4.4. Changes in levels of C1P subspecies in A549 cells by the stable knockdown of CerK

Under our experimental conditions, the major forms of C1P were C24:1 and C24:0 C1P, and the sum of the two C1P species accounted for approximately 70% of total C1P in control A549 cells. Chalfant and coworkers reported that C16:0 C1P was a major form in A549 cells, and the levels of C24:1 C1P varied from 20% to almost equal to that of C16:0 C1P levels in a manner that was dependent on studies and/or experimental conditions [32,50,51]. They showed that different culture conditions, immortalization of cells and cultivation with serum, caused the enhanced formation of C24:1 C1P and C24:0 C1P over those in primary MEFs prepared from CerK-null mice [52]. Thus, these findings and the present results suggest that the levels of C1P subspecies with different *N*-acyl chain lengths varied depending on cellular conditions, including serum. Interestingly, the levels of C18:1 C1P were slightly decreased by the CerK knockdown, while those of other subspecies of C1P and total C1P were not affected under our experimental conditions. The un-change of total C1P levels was also reported in the immortalized MEFs from CerK-null mice [16]. It is reported that the C1P levels in the plasma [52] and neutrophils [53] from CerK-null mice did not change significantly compared to wild-type mice. In contrast, C1P levels are decreased in cells derived from CerK-null mice such as MEF and macrophages, but 50–80% of C1P remains compared to wild-type mice [52]. These results including ours showed that C1P production pathways other than CerK may be the main pathways of C1P production in several cases. In addition, CerK-derived C1P was short-lived and disappeared within 1 h [54], but C1P taken from outside the cell existed for a long time and was hardly metabolized to other lipids after 4 h [55]. These findings suggest that CerK-derived C1P and other pathway-derived C1P exist in different intracellular pools and have different fate and roles. Chalfant's group proposed that the intracellular location of C1P production, not the total amount of C1P in the cell, is the overriding factor of importance in terms of C1P-induced response [32,51]. A contradiction between the unaltered or hardly altered C1P levels and the enhanced migratory responses in A549-shCerK cells may be explained by the localization of CerK in lamellipodia.

4.5. Different migratory responses by the CerK/C1P pathway in literatures and future prospective

In the present study, we showed that the knockdown of CerK in A549 cells enhanced the formation of lamellipodia and cell migration/metastasis. Our results were consistent with previous findings reported by Wijesinghe et al. [16]; they showed the enhanced migration of MEFs prepared from CerK-null mice. Gómez-Muñoz's group also reported that activation of CerK to increase intracellular C1P levels did not cause cell migration in macrophages, unlike when C1P was added extracellularly [12]. An intracellular formation of C1P by its caged analogs stimulated cell proliferation, but not migration, of macrophages [56]. As described above, however, many reports revealed that the extracellular application of C1P caused and/or enhanced cell migration in various cells [11,14,36] and in A549 cells [18]. Under our experimental conditions with serum, an extracellular application of 10 μM C16-C1P increased number of cells having lamellipodia in A549-shLuc cells 30 min after the application; the value with C1P was 30.1 ± 1.1%, which was significantly higher than the control 22.4 ± 2.1% ($P < 0.05$, $n = 3$). In pancreatic cancer cells, both the extracellular addition of C1P and overexpression of CerK caused migration [11]. Gómez-Muñoz's group suggested an involvement of putative C1P receptors on the CerK/C1P-regulated cell migration [12]. The effects of C1P on cell migration may be dependent on many factors such as localization of C1P (extracellular and intracellular C1P), cellular compartments and/or stability of C1P, C1P subspecies, *etc.*, in addition to cell types. A precise analysis is needed in the future to elucidate roles of C1P on cellular functions.

Supplementary data to this article can be found online at https://doi.org/10.1016/j.bbalip.2020.158675.

Author contributions

H. Nakamura, S. Tomizawa, and T. Murayama designed the research; S. Tomizawa, M. Tamori, A. Tanaka, N. Utsumi, and H. Nakamura performed the research; H. Sato, H. Hatakeyama, A. Hisaka, and K. Yamagata assisted the *in vivo* experiments and data analyzing;

T. Kohama, T. Honda, T. Murayama, and H. Nakamura wrote the manuscript.

Transparency document

The Transparency document associated this article can be found, in online version.

Declaration of competing interest

The authors declare no conflict of interest.

Acknowledgements

The analyses of sphingolipids were performed at the Virginia Commonwealth University Lipidomics/Metabolomics Core, supported in part by the NIH-NCI Cancer Center Support Grant P30 CA016059 and by the NIH Grant S10RR031535. This work was supported by JSPS KAKEHNI Grant Number 17K08303 and Hokuto Foundation for Bioscience.

References

[1] S. Bisi, A. Disanza, C. Malinverno, E. Frittoli, A. Palamidessi, G. Scita, Membrane and actin dynamics interplay at lamellipodia leading edge, Curr. Opin. Cell Biol. 25 (2013) 565–573.
[2] S. Jansen, R. Gosens, T. Wieland, M. Schmidt, Paving the Rho in cancer metastasis: Rho GTPases and beyond, Pharmacol. Ther. 183 (2018) 1–21.
[3] C.D. Lawson, A.J. Ridley, Rho GTPase signaling complexes in cell migration and invasion, J. Cell Biol. 217 (2018) 447–457.
[4] A. Sneh, Y.S. Deol, A. Ganju, K. Shilo, T.J. Rosol, M.W. Nasser, R.K. Ganju, Different role of psoriasin (S100A7) in estrogen receptor α positive and negative breast cancer cells occur through actin remodeling, Breast Cancer Res. Treat. 138 (2013) 7727–7739.
[5] N.V. Oleinik, K.L. Helke, E. Kistner-Griffin, N.I. Krupenko, S.A. Krupenko, Rho GTPases RhoA and Rac1 mediate effects of dietary folate on metastatic potential of A549 cancer cells through the control of cofilin phosphorylation, J. Biol. Chem. 289 (2014) 26383–26394.
[6] M. Sugiura, K. Kono, H. Liu, T. Shimizugawa, H. Minekura, S. Spiegel, T. Kohama, Ceramide kinase, a novel lipid kinase, J. Biol. Chem. 277 (2002) 23294–23300.
[7] R.V. Stahelin, P. Subramanian, M. Vora, W. Cho, C.E. Chalfant, Ceramide-1-phosphate binds group IVA cytosolic phospholipase A_2 via a novel site in the C2 domain, J. Biol. Chem. 282 (2007) 20467–20474.
[8] F. Bornancin, Ceramide kinase: the first decade, Cell. Signal. 23 (2011) 999–1008.
[9] D.K. Simanshu, R.K. Kamlekar, D.S. Wijesinghe, X. Zou, X. Zhai, S.K. Mishra, J.G. Molotkovsky, L. Malinina, E.H. Hinchcliffe, C.E. Chalfant, R.E. Brown, D.J. Patel, Non-vesicular trafficking by a ceramide-1-phosphate transfer protein regulates eicosanoids, Nature 500 (2013) 463–467.
[10] N. Presa, A. Gomez-Larrauri, I.G. Rivera, M. Ordoñez, M. Trueba, A. Gomez-Muñoz, Regulation of cell migration and inflammation by ceramide 1-phosphate, Biochim. Biophys. Acta 186 (2016) 402–409.
[11] I.G. Rivera, M. Ordoñez, N. Presa, P. Gangoiti, A. Gomez-Larrauri, M. Trueba, T. Fox, M. Kester, A. Gomez-Muñoz, Ceramide 1-phosphate regulates cell migration and invasion of human pancreatic cancer cells, Biochem. Pharmacol. 102 (2016) 107–119.
[12] M.H. Granado, P. Gangoiti, A. Ouro, L. Arana, M. González, M. Trueba, A. Gómez-Muñoz, Ceramide 1-phosphate (C1P) promotes cell migration: involvement of a specific C1P receptor, Cell. Signal. 21 (2009) 405–412.

[13] G. Schneider, E. Bryndza, A. Abdel-Latif, J. Ratajczak, M. Maj, M. Tamowski, Y.M. Klyachkin, P. Houghton, A.J. Morris, A. Vater, S. Klussmann, M. Kucia, M.Z. Ratajczak, Bioactive lipids S1P and C1P are prometastatic factors in human rhabdomyosarcoma, and their tissue levels increase in response to radio/chemotherapy, Mol. Cancer Res. 11 (2013) 793–807.
[14] C. Kim, S. Schneider, A. Abdel-Latif, K. Mierzejewska, M. Sunkara, S. Borkowska, J. Ratajczak, A.J. Morris, M. Kucia, M.Z. Ratajczka, Ceramide-1-phosphate regulates migration of multipotent stromal cells and endothelial progenitor cells: implications for tissue regeneration, Stem Cells 31 (2013) 500–510.
[15] A.W. Payne, D.K. Pant, T.C. Pan, L.A. Chodosh, Ceramide kinase promotes tumor cell survival and mammary tumor recurrence, Cancer Res. 74 (2014) 6352–6363.
[16] D.S. Wijesinghe, M. Brentnall, J.A. Mietla, L.A. Hoeferlin, R.F. Diegelmann, L.H. Boise, C.E. Chalfant, Ceramide kinase is required for a normal eicosanoid response and the subsequent orderly migration of fibroblasts, J. Lipid Res. 55 (2014) 1298–1309.
[17] A. Hsu, W. Zhang, J.F. Lee, J. An, P. Ekambaram, J. Liu, K.V. Honn, C.M. Kling, M.J. Lee, Sphingosine-1-phosphate receptor-3 signaling up-regulates epidermal growth factor receptor and enhances epidermal growth factor receptor-mediated carcinogenic activities in cultured lung adenocarcinoma cells, Int. J. Oncol. 40 (2012) 1619–1626.
[18] G. Schneider, Z.P. Sellers, K. Bujko, S.S. Kakar, M. Kucia, M.Z. Ratajczak, Novel pleiotropic effects of bioactive phospholipids in human lung cancer metastasis, Oncotarget 8 (2017) 58247–58263.
[19] S. Sarkar, M. Maceyka, N.C. Hait, S.W. Paugh, H. Sankala, S. Milstien, S. Spiegel, Sphingosine kinase 1 is required for migration, proliferation and survival of MCF-7 human breast cancer cells, FEBS Lett. 579 (2005) 5313–5317.
[20] F. Döll, J. Pfeilschifter, A. Huwiler, The epidermal growth factor stimulates sphingosine kinase-1 expression and activity in the human mammary carcinoma cell line MCF7, Biochim. Biophys. Acta 1738 (2005) 72–81.
[21] K.A. Orr Gandy, M. Adada, D. Canals, B. Carroll, P. Roddy, Y.A. Hannun, L.M. Obeid, Epidermal growth factor-induced cellular invasion requires sphingosine-1-phosphate/sphingosine-1-phosphate 2 receptor-mediated ezrin activation, FASEB J. 27 (2013) 3155–3166.
[22] M.M. Adada, D. Canals, N. Jeong, A.D. Kelkar, M. Hernandez-Corbacho, M.J. Pulkoski-Gross, J.C. Donaldson, Y.A. Hannun, L.M. Obeid, Intracellular sphingosine kinase 2-derived sphingosine-1-phosphate mediates epidermal growth factor-induced ezrin-radixin-moesin phosphorylation and cancer cell invasion, FASEB J. 29 (2015) 4654–4669.
[23] S. Nishino, H. Yamashita, M. Tamori, M. Mashimo, K. Yamagata, H. Nakamura, T. Murayama, Translocation and activation of sphingosine kinase 1 by ceramide-1-phosphate, J. Cell. Biochem. 120 (2019) 5396–5408.
[24] C. Graf, M. Klumpp, M. Habig, P. Rovina, A. Billich, T. Baumruker, B. Oberhauser, F. Bornancin, Targeting ceramide metabolism with a potent and specific ceramide kinase inhibitor, Mol. Pharmacol. 74 (2008) 925–932.
[25] S.C. Mills, L. Howell, A. Beekman, L. Stokes, A. Mueller, Rac1 plays a role in CXCL12 but not CCL3-induced chemotaxis and Rac1 GEF inhibitor NSC23766 has off target effects on CXCR4, Cell. Signal. 42 (2018) 88–96.
[26] E. Tada, K. Toyomura, H. Nakamura, H. Sasaki, T. Saito, M. Kaneko, Y. Okuma, T. Murayama, Activation of ceramidase and ceramide kinase by vanadate via a tyrosine kinase-mediated pathway, J. Pharmacol. Sci. 114 (2010) 420–432.
[27] T. Kato, H. Fujino, S. Oyama, T. Kawashima, T. Murayama, Indomethacin induces cellular morphological change and migration via epithelial-mesenchymal transition in A549 human lung cancer cells: a novel cyclooxygenase-inhibition-independent effect, Biochem. Pharmacol. 82 (2011) 1781–1791.
[28] S. Suzuki, A. Tanaka, H. Nakamura, T. Murayama, Knockout of ceramide kinase aggravates pathological and lethal responses in mice with experimental colitis, Biol. Pharm. Bull. 41 (2018) 797–805.
[29] J.V. Small, T. Stradal, E. Vignal, K. Rottner, The lamellipodium; where motility begins, Trends Cell Biol. 12 (2002) 112–120.
[30] S. Mezi, L. Todi, E. Orsi, A. Angeloni, P. Mancini, Involvement of the Src-cortactin pathway in migration induced by IGF-1 and EGF in human breast cancer cells, Int. J. Oncol. 41 (2012) 2128–2138.
[31] P. Mitra, M. Maceyka, S.G. Payne, N. Lamour, S. Milstien, C.E. Chalfant, S. Spiegel, Ceramide kinase regulates growth and survival of A549 human lung adenocarcinoma cells, FEBS Lett. 581 (2007) 735–740.
[32] N.F. Lamour, R.V. Stahelin, D.S. Wijesinghe, M. Maceyka, E. Wang, J.C. Allegood, A.H. Merrill Jr., W. Cho, C.E. Chalfant, Ceramide kinase uses ceramide provided by ceramide transport protein: localization to organelles of eicosanoid synthesis, J. Lipid Res. 48 (2007) 1293–1304.
[33] Y.H. Zeidan, R.W. Jenkins, Y.A. Hannun, Remodeling of cellular cytoskeleton by the acid sphingomyelinase/ceramide pathway, J. Cell Biol. 181 (2008) 335–350.
[34] M.D. Hansen, W.J. Nelson, Serum-activated assembly and membrane translocation of an endogenous Rac1:effector complex, Curr. Biol. 11 (2001) 356–360.
[35] A. Payapilly, A. Malliri, Compartmentalisation of RAC1 signaling, Curr. Opin. Cell Biol. 54 (2018) 50–56.
[36] J.L. Hankins, K.E. Ward, S.S. Linton, B.M. Barth, R.V. Stahelin, T.E. Fox, M. Kester, Ceramide 1-phosphate mediates endothelial cell invasion via the annexin a2-p11 heterotetrameric protein complex, J. Biol. Chem. 288 (2013) 19726–19738.
[37] S. Das, T. Yin, Q. Yang, J. Zhang, Y.I. Wu, J. Yu, Single-molecule tracking of small GTPase Rac1 uncovers spatial regulation of membrane translocation and mechanism for polarized signaling, Proc. Natl. Acad. Sci. U. S. A. 112 (2015) E267–E276.
[38] M.C. Caino, C. Lopez-Haber, J.L. Kissil, M.G. Kazanietz, Non-small cell lung carcinoma cell motility, Rac activation and metastatic dissemination are mediated by protein kinase C epsilon, PLoS ONE 7 (2012) e31714.
[39] T.J. Kim, S. Mitsutake, Y. Igarashi, The interaction between the pleckstrin homology domain of ceramide kinase and phosphatidylinositol 4,5-bisphosphate regulates the plasma membrane targeting and ceramide 1-phosphate levels, Biochem. Biophys. Res. Commun. 342 (2006) 611–617.
[40] H. Yamaguchi, J. Condeelis, Regulation of the actin cytoskeleton in cancer cell migration and invasion, Biochim. Biophys. Acta 1773 (2007) 642–652.
[41] S.H. Xia, J. Wang, J.X. Kang, Decreased *n-6/n-3* fatty acid ration reduces the invasive potential of human lung cancer cells by downregulation of cell adhesion/invasion-related genes, Carcinogenesis 26 (2005) 779–784.
[42] J.I. Kim, V. Lakshmikanthan, N. Frilot, Y. Daaka, Prostaglandin E_2 promotes lung cancer cell migration via EP4-βarrestin-c-Src signalsome, Mol. Cancer Res. 8 (2010) 569–577.
[43] M.F. Bijlsma, K.S. Borensztajn, H. Roelink, M.P. Peppelenbosch, C.A. Spek, Sonic hedgehog induces transcription-independent cytoskeletal rearrangement and migration regulated by arachidonate metabolites, Cell. Signal. 19 (2007) 2596–2604.
[44] M.J. Kim, H.S. Kim, S.H. Lee, Y. Yang, M.S. Lee, J.S. Lim, NDRG2 controls COX-2/PGE_2-mediated breast cancer cell migration and invasion, Mol. Cell 37 (2014) 759–765.
[45] H. Nakamura, T. Hirabayashi, M. Shimizu, T. Murayama, Ceramide-1-phosphate activates cytosolic phospholipase $A_2\alpha$ directly and by PKC pathway, Biochem. Pharmacol. 71 (2006) 850–867.
[46] Y.X. Wang, H. Lv, Z.X. Li, C. Li, X.Y. Wu, Effect of shRNA mediated down-regulation of annexin A2 on biological behavior of human lung adenocarcinoma cells A549, Pathol. Oncol. Res. 18 (2012) 183–190.
[47] M.H. Granado, P. Gangoiti, A. Ouro, L. Arana, A. Gómez-Muñoz, Ceramide 1-phosphate inhibits serine palmitoyltransferase and blocks apoptosis in alveolar macrophages, Biochim. Biophys. Acta 1791 (2009) 263–272.
[48] M. Suzuki, K. Cao, S. Kato, Y. Komizu, N. Mizutani, K. Tanaka, et al., Targeting ceramide synthase 6-dependent metastasis-prone phenotype in lung cancer cells, J. Clin. Invest. 126 (2016) 254–265.
[49] L. Camacho, Ó. Meca-Cortés, J.L. Abad, S. García, N. Rubio, A. Díaz, T. Celiá-Terrassa, F. Cingolani, R. Bermudo, P.L. Fernández, J. Blanco, A. Delgado, J. Casas, G. Fabriás, T.M. Thomson, Acid ceramidase as a therapeutic target in metastatic prostate cancer, J. Lipid Res. 54 (2013) 1207–1220.
[50] N.F. Lamour, P. Subramanian, D.S. Wijesinghe, R.V. Stahelin, J.V. Bonventre, C.E. Chalfant, Ceramide 1-phosphate is required for the translocation of group IVA cytosolic phospholipase A_2 and prostaglandin synthesis, J. Biol. Chem. 284 (2009) 26897–26907.
[51] D.S. Wijesinghe, J.C. Allegood, L.B. Gentile, T.E. Fox, M. Kester, C.E. Chalfant, Use of high performance liquid chromatography-electrospray ionization-tandem mass spectrometry for the analysis of ceramide-1-phosphate levels, J. Lipid Res. 51 (2010) 641–651.
[52] J.A. Mietla, D.S. Wijesinghe, L.A. Hoeferlin, M.D. Shultz, R. Natarajian, A.A. Fowler 3rd, C.E. Chalfant, Characterlization of eicosanoid synthesis in a genetic ablation model of ceramide kinase, J. Lipid Res. 54 (2013) 1834–1847.
[53] C. Graf, B. Zemann, P. Rovina, N. Urtz, A. Schanzer, R. Reuschel, et al., Neutropenia with impaired immune response to *Streptococcus pneumoniae* in ceramide kinase-deficient mice, J. Immunol. 180 (2008) 3457–3466.
[54] A. Boath, C. Graf, E. Lidome, T. Ullrich, P. Nussbaumer, F. Bornancin, Regulation and traffic of ceramide 1-phosphate produced by ceramide kinase: comparative analysis to glucosylceramide and sphingomyelin, J. Biol. Chem. 283 (2008) 8517–8526.
[55] P. Gangoiti, C. Bernacchioni, C. Donati, F. Cencetti, A. Ouro, A. Gómez-Muñoz, P. Bruni, Ceramide 1-phosphate stimulates proliferation of C2C12 myoblasts, Biochimie 94 (2012) 597–607.
[56] A. Gomez-Muñoz, P. Gangoiti, I.G. Rivera, N. Presa, A. Gomez-Larrauri, M. Ordoñez, Caged ceramide 1-phosphate (C1P) analogs: novel tools for studying C1P biology, Chem. Phys. Lipids 194 (2016) 79–84.